

A Spatiotemporal Approach in Detecting and Analyzing Hydro-climatic Change in Northwest Algeria

Sarra Bouraoui

Laboratory for Research and Studies in Planning and Urban
Planning (LREAU)
University of Sciences and Technology Houari Boumediene
Algiers, Algeria
bouraouisarrahydraule@gmail.com

Abderrahmane Medjerab

Laboratory for Research and Studies in Planning and Urban
Planning (LREAU)
University of Sciences and Technology Houari Boumediene
Algiers, Algeria
a.medjerab@gmail.com

Received: 15 September 2022 | Revised: 26 September 2022 | Accepted: 27 September 2022

Abstract—Understanding climatic behavior, particularly that of semi-arid regions, is essential in order to optimize water resources management and provide protection from climatic risks. Water resources have great socio-economic and environmental importance. This paper focuses on the statistical analysis of the rainfall regime of northwest Algeria and estimates its spatial distribution and temporal variation. To this end, time series and principal component analysis were performed on rainfall series recorded from 1913 to 2009, representing the annual precipitation from thirty meteorological stations to discover patterns and trends in the studied region. Furthermore, the applied spectral analysis of the time series reveals the existence of a period of approximately 97 years at all stations. ArcGIS along with statistical and analytical tools like SPSS and XLSTAT were utilized in this study of the climatic behavior in northwest Algeria.

Keywords—rainfall series; statistics analysis; cartography; spectral analysis; climate variability

I. INTRODUCTION

Learning about climatic behavior in a region improves hydraulic constructions and plays a critical part in the management of water resources in various term lengths [1]. Researchers are trying to answer questions such as if there is there a climate change in the study region and how can the existence of any change be confirmed. In response to these complex questions, a verification of climate change parameters is required, such as the temporal homogeneity of hydro-meteorological time series, in particular stating the presence of trends in the case of annual rainfall series. Numerous studies analyze the variability of precipitation in the Mediterranean Basin and African regions. Linear trends from 1901–2005 show high spatial variability [2]. In comparison to other regions, positive annual precipitation trends were detected in North and South America, the Eurasian continent, and Australia. On the other hand, several observations were made concerning a significant decrease in annual totals in Western Africa, Sahel, the Western Coast of South America, and the

Mediterranean Basin [2]. In the zone of Sahel, there are several indicators of decreasing trend in rainfall series from 1970 to 1990 [3-7]. Consequently, it was observed that alteration in climatic parameters can result in modification of the hydrological cycle which affects the quantity and quality of rainfall and water resources [8]. The drought affected other countries around the Gulf of Guinea in the late '60s [9-11] and altered the rainfall regime of Sahel from 1990 to 2007, increasing it by 10% in comparison with the rainfall regime of the 1970–1989, but it was still lower than the 1950–1989 average (a 20-year wet period (1950-1969) and 20-year dry period (1970-1989)). While the rainfall deficit continued in Western Sahel, Central Sahel gradually recorded more wet years beginning from the late 1990s, but the recovery was considerably limited (1990-2007). As a conclusion, there are numerous differences between Western and Central Sahel regarding the inter-annual variability pattern and the seasonal cycle.

In Mediterranean regions, several researchers have observed a decrease in annual precipitation. Yearly and seasonal precipitation series from 32 stations from 1833 to 1996 were examined in [12]. Declining trends in several yearly series were noticed, which were remarkable, considering the statistics, only in Southern Italy. On a seasonal basis, a declining trend was significant only during spring in Southern Italy and autumn in Northern Italy. In Southern Italy (Calabria), statistical analysis of annual and seasonal precipitation on 109 series with over 50 years of processed data was performed in [13]. The rainfall data segment was first calculated following a pre-whitening technique to lower the autocorrelation of the rainfall series. The study showed a decreasing trend for annual and winter fall rainfall and an increasing trend for summer rainfall. In addition, raised percentages of rainfall series show breaks during the 1960-1970 period. Nonetheless, the analysis on parts of the Mediterranean area shows that the surging progression is a non-considerable reduction in precipitation or a lack of linear trend during the last century or a shorter period [14-16].

Corresponding author: Sarra Bouraoui

www.etasr.com

Bouraoui & Medjerab: A Spatiotemporal Approach in Detecting and Analyzing Hydro-climatic Change ...

A study of the changes in data series of climate variables at annual and monthly scales in the western part of the French Mediterranean area showed that annual precipitation was too low [17]. Moreover, the study stated that monthly rainfalls were decreasing in June and increasing in November throughout the area. The changes in precipitation of the Balearic Islands (Spain) were studied in [18], considering the daily time series from the 1951-2006 period, confirming a negative trend of annual precipitation. An abrupt decrease in a year's rainfall of 65mm has been identified in the time series around 1980.

In the current study, spatiotemporal analysis of precipitation with a set of statistical methods is used to recognize trends and identify break dates and spatial patterns of precipitation variability of the southern Mediterranean region. For this purpose, a series representing the total annual precipitation of approximately 30 stations in Western Algeria, with the recorded data spreading over a period of 97 years (1913-2009) were examined. The data were analyzed with the use of the Spearman test for the detection of trends, the Mann-Kendall and Pettitt tests for the detection and localization of these trends, spectral analysis to study the nature of the variations, and Principal Component Analysis (PCA) to identify regions of consistent precipitation variability [8].

II. STUDY AREA AND PRECIPITATION DATA

The considered region extends between the meridians -2° West and 1° east, and between the North $36^{\circ}33'$ and $33^{\circ}91'$. It includes the catchments of Cheliff (01), Oraneese coast (04), Mactan (11), and Tafna (16) (the numbers in parentheses indicate catchment codes). The area is bordered in the north by the Mediterranean Sea, in the west by the Algerian-Moroccan borders, in the south by high plains, and in the east by the mountainous massif of Ouarsenis.

In Algeria, the climate of the northwest is affected by diverse factors, such as the atmospheric circulation and topography. From December to February, the winds are directed west-northwest. These winds must cross the narrow arm of the sea that distinguishes the study area from Spain, to access northwestern Algeria. Before leaving Spain, the winds discharge part of their moisture on the high peaks of the Sierra Nevada. The air masses do not have enough time to accumulate sufficient water vapor and reach northwestern Algeria relatively dry. During their journey over the Mediterranean Sea, the water-laden easterly winds favor the appearance of heavy precipitation, but this occurs rarely during the winter. Heterogeneity characterizes the area. West Tellian Atlas has a fragmented relief. The high west plains are arid steppes.

In Morocco, the Middle Atlas Rif Ridge protects northwestern Algeria. It exposes a complex topography with a split mountainous character, which increases the areas of shelter while the exposure to sea influences and disturbs flows. Figure 2 shows the location and geographical features of the region. The aforementioned factors contribute to the lowering of the precipitation and consequently to the surface and subsurface water resources.

The atmospheric circulation forms the climate of northwest Algeria and is composed of cells with latitudinal extensions. Among these cells, we can mention the following:

- The Azores High, a zone with permanent high pressure that grows in the middle of the Atlantic, in the region of the Azores Islands. Its propagation to the Maghreb area deflects the meteorological troubles towards Europe.
- The Saharan anticyclone is much more stable than the previous anticyclone from the general circulation point of view.

Irregularity is the most important index of precipitation: spatial and temporal irregularity from one region to another, eminently an inter-annual irregularity. Sometimes, heavy rainfalls cause catastrophic floods. Most of the region has precipitation totals between 200 and 800mm. The southwestern zone is the driest, with the lowest annual rate of 100mm. Another significant aspect is the low number of rainy days (between 14% and 21%).

The rainfall data were provided by the National Agency of Hydraulic Resources (ANRH). The original database comprises daily precipitation records from 30 stations distributed throughout the area, covering various periods with more than 97 years of observations. Analysis of precipitation variability requires long data sets in excellent condition. In addition, analyzing the spatial distribution of a general term in all stations should be chosen carefully. For this reason, we had to balance the length of the periods and the number of included stations. The number of missing data records influences precipitation analysis, so only series with $< 10\%$ missing values were maintained.

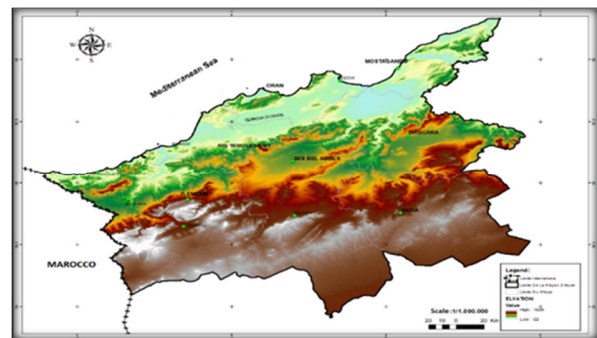


Fig. 1. Elevation map of western Algeria with principal mountains (2020).

The quality controls on the selected data sets had two main steps, the first of which was to discover possible errors and suspect precipitation records. In the second step, the data sets were subject to a homogeneity test. Data homogenization helps conceive observations conditionally, so the temporal variations of the adjusted data are only brought in by the climatic processes. The most frequent causes of the lack of homogeneity of the climatic data are the changes in the location of the stations, alterations in screen designs, or environmental changes around the station. The cumulative residuals had to be tested to detect such anomalies in the series. The test allows for a qualitative evaluation at a given significance level of the

homogeneity of the precipitation series concerning the confirmed homogeneous series by comparing the packed residuals of linear regression with an elliptical confidence interval (Bois ellipse). Only series that did not show heterogeneities were selected. Finally, 30 annual precipitation time series passed the above described quality control, which were also acceptably distributed throughout the study area, covering the 1913–2009 time period, and missing less than 10% values (Figure 2). The missing values were interpolated by linear regression based on a series from adjacent stations. Linear regression equations were established separately with complete series of 1 or 4 adjacent stations as independent variables and incomplete series as the dependent variable. The relative error in evaluating the interpolation was obtained by averaging 5 relative errors calculated from 5 observed and predicted values near the missing data. The linear regression equation with the lowest relative error rate was the chosen equation for predicting the missing data. The maximum relative error did not exceed 15%.

III. METHODOLOGY

Several parametric and nonparametric tests were used for trend detection. Parametric trend tests are more cumbersome than nonparametric tests, which require independent and properly distributed data. In contrast, nonparametric tests require only independent data and may allow for outliers. To detect trends in the precipitation time series, we decided to use nonparametric tests that overcome the obstacles of other methods. Mann–Kendall test [19, 20] and Spearman’s test are widely used to detect trends in time series. Their efficiency and power have been proven significant in similar applications [21]. Additionally, when implemented in a sequential version, the Mann-Kendall test positions itself notably well in synchronization with the trend appearance. To reinforce the results of both tests, we performed another nonparametric test, the Pettitt test, which can detect the breakpoint of serial average at any level of significance. It designates a highly precise magnitude of the detected trend. Spectral analysis helps determine the periodicities in the precipitation time series [22]. Afterward, principal component analysis is applied to deduce a spatiotemporal regionalization of the precipitation variability.

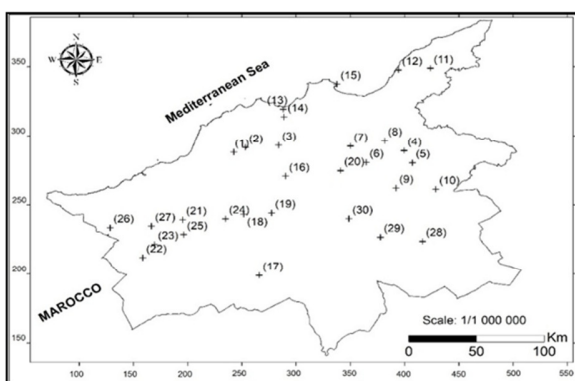


Fig. 2. Station positions in the study area.

IV. SPEARMAN’S TEST

Spearman’s test is a rank-based nonparametric statistical test that can be used to detect monotonic trends in a time series [23, 24]. The Spearman test was used to analyze hydro-meteorological trends in [25-27].

For a given sample of data ($X_i, i = 1, 2, \dots, N$), the null hypothesis H_0 states that all X_i are independent and identically distributed. The alternative hypothesis is that X_i increases or decreases with i , i.e. there is a trend. The test’s statistics are given as [24]:

$$r_s = 1 - \frac{6}{N(N^2-1)} \sum_{i=1}^N (y_i - i)^2 \quad (1)$$

where y_i is the rank of the i -th observation X_i in a sample of size N .

The diffusion of this statistic is asymptotically correct under the null hypothesis with the mean and variance of (2) and (3):

$$E(r_s) = 0 \quad (2)$$

$$\text{var}(r_s) = \frac{1}{N-1} \quad (3)$$

The exceedance probability a_1 is computed using the normal cumulative distribution function with zero mean and variance $\text{var}(r_s)$:

$$a_1 = P(|u| > |u(r_s)|) \quad (4)$$

$$u(r_s) = r_s \sqrt{N-1} \quad (5)$$

Then, the null hypothesis is adopted or not at a significance level of 0 depending on whether $a_1 > a_0$ or $a_1 < a_0$. Significant values of $|r_s|$ show a decreasing or increasing trend.

V. MANN–KENDALL TEST

The Mann–Kendall test is also a rank-based nonparametric test which associates a number n_i to each x_i where x_i is the number of elements, such that $i > j$, and $x_i > x_j$. Mann-Kendall statistic is:

$$t = \sum_{i=1}^N y_i \quad (6)$$

Under the null hypothesis, the statistic is, for a large sample, normally distributed with mean and variance assigned by:

$$E(t) = \frac{N(N-1)}{4} \quad (7)$$

$$E(t) = \frac{N(N-1)}{4} \quad (8)$$

Its reduced form is:

$$U(t) = \frac{t-E(t)}{\sqrt{\text{var}(t)}} \quad (9)$$

The null hypothesis is unacceptable for high values of the reduced statistic. Positive values of $U(t)$ indicate increasing trends, while negative values show decreasing trends. When testing either increasing or decreasing monotonic trends at a significance level, the null hypothesis was rejected for an absolute value of $U(t)$ greater than $U_{1-\alpha/2}$, and $U_{1-\alpha/2}$ is the critical value obtained from the standard normal cumulative distribution tables. In this research, a significance level of 0.05

was applied. The sequential version of the test (in a forward and a backward sense) enables us to identify the star to trend within the data series. Note that $U(t)$ is the forward sequence. The backward sequence $U'(t)$ is studied with the same function but with the opposite data series. In the absence of any trend, the graphical representation of the curves $U(t)$ and $U'(t)$ overlap many times. When the null hypothesis is rejected (i.e. when any of the points in $U(t)$ exceeds the confidence interval ± 1.96), an increasing or decreasing trend is indicated. The test statistic applied in this study allows finding the approximate moment of the appearance of the trend by locating the intersection of the curves $U(t)$ and $U'(t)$. A point of intersection with the confidence interval shows a point of change. The parts of the curves ahead of the confidence lines show the time domain of a sudden change. Detailed descriptions of this nonparametric test can be found in [24].

VI. PETTITT TEST

The Pettitt test is a nonparametric test derived from the Mann–Whitney test [28]. The absence of a break constitutes the null hypothesis. Pettitt defines the variable $U_{t,N}$ as:

$$U_{t,N} = \sum_{i=1}^t \sum_{j=i+1}^N \text{Sgn}(z) \quad (10)$$

$$Z = X_i - X_j \quad (11)$$

where $\text{Sgn}(z) = 1$ if $z > 0$, 0 if $z = 0$ and -1 if $z < 0$.

He suggested testing the null hypothesis by using the statistic K_N defined by the maximum value of $U_{t,N}$ for $t=1, \dots, N-1$. From the rank theory, Pettitt demonstrates that if k indicates a value of the K_N series, under the null hypothesis, the exceedance probability of the k value is given by:

$$\text{Prob}(K_N > k \approx 2 \exp(-6K^2/(N^3 + N^2))) \quad (12)$$

For a type I error α , if the exceedance probability estimated is less than α , the null hypothesis is rejected. The time series demonstrate a trend at time t where the K_N appears.

VII. PRINCIPAL COMPONENT ANALYSIS

PCA is a classical factorial procedure. It changes several (possibly) correlated variables (here, the annual precipitation stations) into a (smaller) number of synthetic uncorrelated variables called Principal Components (PCs). Every time series (factor score) is linked to a component. PCA ensures the detection of coherent and recurring modes in the total domain. Rotation methods allow us to improve the interpretability of the results through a linear transformation of the PC. Compared to the non-rotated solution, orthogonal rotations (preserving the correlation between the PCs) are less affected by the domain form, and the instability of the subdomain (the fact that the PCA is performed only on a part of the field leads to different results from those of the PCA of the entire field) and the sampling errors between the PCs. Varimax is the most commonly used rotation [29]. Its goal is to maximize the variance of the factorial weights between each component for a given variable, increasing the segregation between the various PCs.

VIII. SPECTRAL ANALYSIS

The spectral density takes the frequency content of a stochastic process and allows the identification of periodicities. The spectral density function resembles the passage from a temporal mode to a frequency mode by a Fourier modification of the autocorrelation function. The interpretation of the spectral density function, $S(f)$, through the recognition of the different peaks indicating periodic phenomena, leads to the characterization of the system:

$$S(f) = 2[1 + 2 \sum_{k=1}^m D(k)r(k) \cos(2\pi fk)] \quad (13)$$

$$D(k) = \frac{(1 + \cos \frac{k}{m})}{2} \quad (14)$$

where $j=1$ to m , f is the frequency and $D(k)$ ensures that the estimated values $S(f)$ are not biased (Tukey filter). $r(k)$ is the autocorrelation function expressed by:

$$r(k) = \frac{C(k)}{C(0)} \quad (15)$$

$$C(k) = \frac{1}{n} \sum_{t=1}^{n-k} (x_t - \bar{X})(x_{t+k} - \bar{X}) \quad (16)$$

where k is the time lag ($k = 1 \dots m$), n is the length of the time series, x is a single event, \bar{X} is the mean of the events and m is the cutting point. The cutting point is usually determined based on the interval of the analysis and the given circumstances.

IX. RESULTS AND DISCUSSION

A. Temporal Analysis

Spearman and Mann–Kendall tests were applied to the data series of annual rainfalls of the 30 selected stations and a significantly decreasing trend was detected at a significance level of 5% for 29 stations (Figure 3). Only the Ghriba station, in the eastern zone of the studied domain, presents a significantly increasing trend at a 5% level. In the region, this station is behind an isolated station.

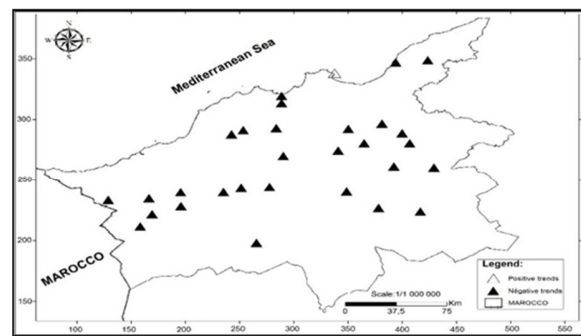


Fig. 3. Trends in annual total precipitation during 1914–2004 detected by the Mann–Kendall method.

The curves overlap (e.g. Figure 4(a) for Mostaganem 1 station) and the statistical values do not surpass the limits of the critical significance levels, except for the series of Youb that present significant statistic variations, indicating the presence of dry periods. The intersection point between both curves (forward and backward) within the confidence interval demonstrates the change point that compares to the break date.

The graph in Figure 4(b) shows the forward and backward results of the test for the Youb station. The intersection of the two curves marks a change that occurred in 1955. The evident results obtained previously and the location of the break years in different levels of significance is provided by analyzing the whole series with the Pettit Test. Evidently, the results show that an abrupt change (decrease in rainfall) within the time series is observed mainly from the end of the 1940s until the beginning of the 1950s. For 6 stations, the beginning of the trend was detected between 1953 and 1980, 26 stations led to a very significant decreasing trend between 1975 and 1996, and the others appeared to be stationary and confirmed the previous results. Hence, the presence of a rainfall deficit is evident in the eastern zone from the beginning of the 1930s and accentuated during the 1950s and 1970s by its extension to the whole region.

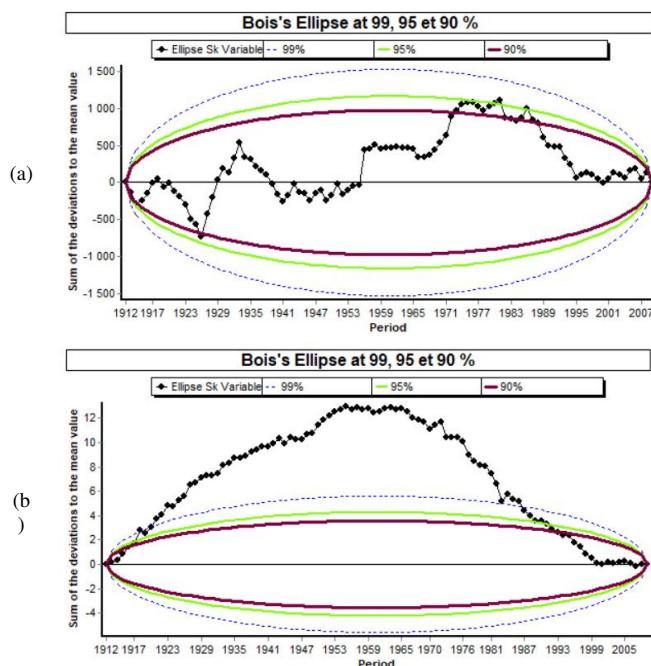


Fig. 4. Mann-Kendall progressive test applied to stations: (a) Mostaganem I, (b) Youb.

Trends can be detected using Pettitt's and Mann-Kendall's tests. However, these tests cannot find more than one break date. This represents the drawback of these tests when investigating rainfall time series, which could have multiple increasing and decreasing trends and/or breaks, specifically for long series. When the number of stations used is not very large, a limit is triggered by the difficulty of interpreting the results on a regional scale. These results suggest that further investigation is needed. We tried to perform spectral density analysis to seek possible periodicities and supplementary PCA was carried out, and regionalization of rainfall variability was performed.

B. Spatiotemporal Rainfall Variability

PCA was applied with the stations as variables and the 97 annual precipitation values. The analysis without and with

rotation underlines that the first 4 components account for most of the total variance (57.8%), as shown in Table I.

TABLE I. EXPLAINED VARIANCES BY THE FOUR FIRST PCs BEFORE AND AFTER ROTATION (F: FACTORS)

	PC (without rotation)				RPC (rotated)			
	F1	F2	F3	F4	F1	F2	F3	F4
Variance %	45.988	6.575	5.250	4.830	29.292	14.156	5.049	14.147
Cumulative variance %	45.988	52.563	57.813	62.643	29.292	43.448	48.496	62.643

The first component accounts for a large part of the variance (45.988%). It describes the inter-annual variability of the precipitation for the whole region (opposing humid and dry years). All stations are correlated positively with this component, considering varying coefficients between 0.85 and 0.2. The greatest coefficients are noted in the deepest region (Figure 5). The objective of the test here is to identify regions with the same variation mode. This geographical consistency can be justified by the large homogeneity of the weather regimes (winter rains and summer drought), but it denotes that a long stretch of years presents large deficits or excesses over the whole region. The observation complies with the result that is found by the nonparametric statistical test of trend detection, as shown above.

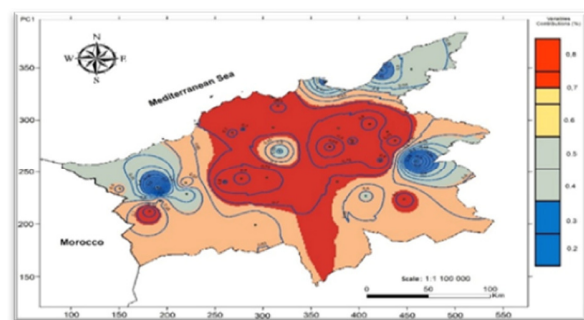


Fig. 5. Spatial distribution of the first PC (PC1) fields in the area of study (PCA without rotation).

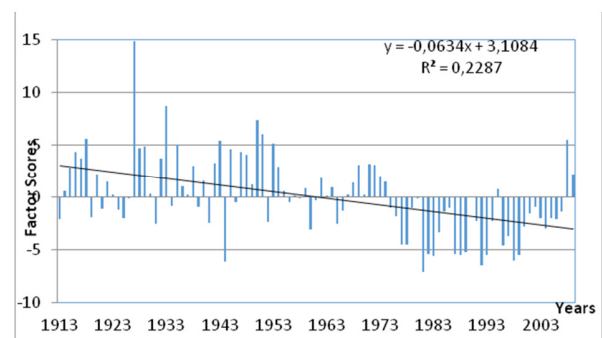


Fig. 6. Temporal factorial scores of PC1 without rotation. The straight line represents the chronicle trend.

The time series of the amplitudes of the first component (Figure 6) highlights wet years (1927, 1933, and 1950) and the succession of dry years that most stations of the region recorded. A decreasing trend with a significant determination

coefficient of 0.2287 is clear starting from the end of 1975 to 2007 (with an absolute minimum in 1981).

The following components (Figure 7) account for smaller proportions of the variance. The second component accounts for only 6.575% of the variance (Table I). It shows opposite amplitudes between parts of the eastern region correlated positively (heavy rainfall) and the west and southwest (areas affected by the Foehn phenomenon. The distance from the sea influences the rainfall flows and, therefore these areas have low rainfall). The third component shows 5.25% of the variance. It represents the southwest and southern parts to the north and center of the study area. The first component accounts for the largest amount of total variance, however, some stations are correlated with this component. We performed a rotation of the factorial axes according to the Varimax method. Varimax orthogonal rotation is the option used to avoid some of the domain shape dependences [29] and to obtain a stable and physically meaningful pattern. The principle is to determine the components that correlate best with the variables [16, 30].

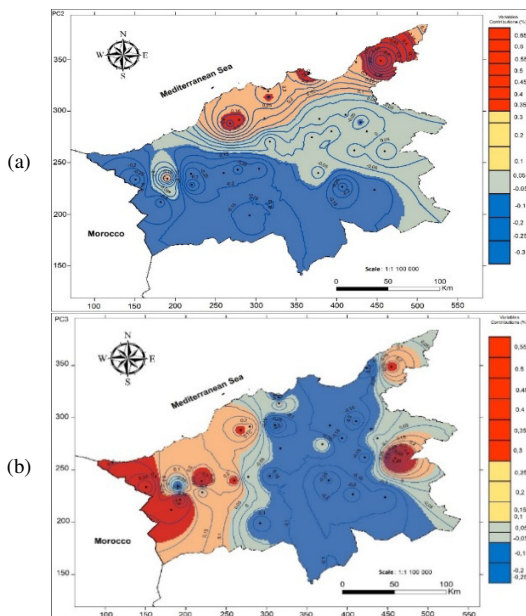


Fig. 7. Spatial distribution of (a) PC2 and (b) PC3 fields in the study area (PCA without rotation).

We retained the first 4 components accounting for 62.643% of the variance. The percentage of variance demonstrated by the eigenvalues is different from the PCA without rotation, with less variance demonstrated by the first component and more variance detailed by the other models. The first component shows the western and central parts of the region (coastal plains). The stations most related to this component are those with elevations between 5 and 215m. The eastern region is known for its low relief and low precipitation (annual rainfall <500mm) with a weakly explained variability (variation coefficients <0.30), see Figure 8(a).

The second component characterizes the eastern part of the study area (Dahra Mountains). This region is well-watered, expressing the simultaneous influence of topography and

atmospheric circulation on rainfall (Figure 8(b)). The third component characterizes the variability of the western part of the study region (Figure 8(c)). The fourth component represents the Tellian Plateau and the high plains in the east, characterized by weak rainfall with a low estimate of 450mm and a very sporadic character due to the shelter effect that reduces the influence of the rainy systems covering the west and northwest (Figure 8(d)).

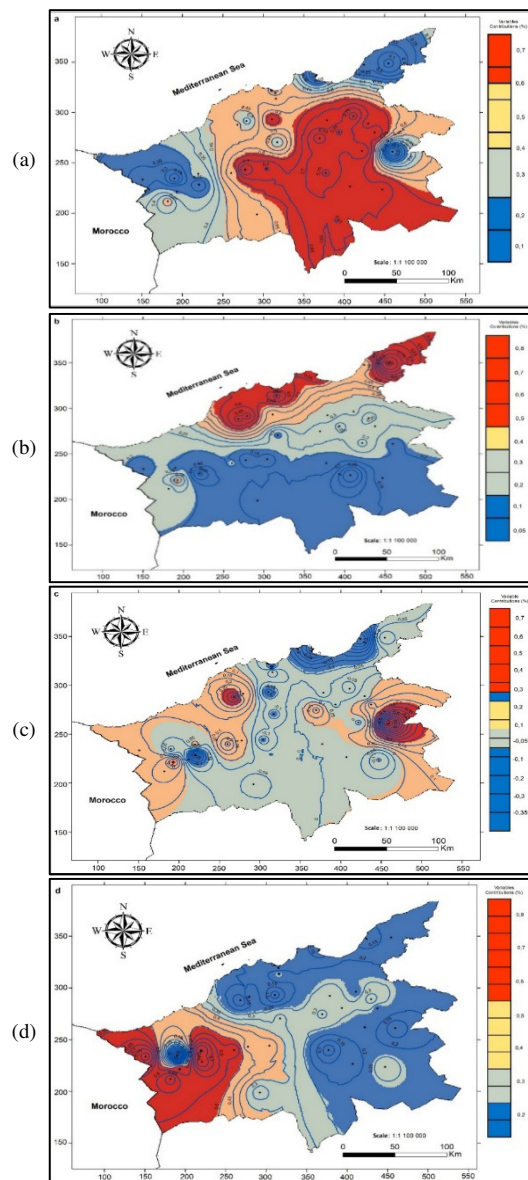


Fig. 8. Spatial distribution of (a) PC1, (b) PC2, (c) PC3, (d) PC4 fields in the study area (PCA with Varimax rotation).

The time series associated with the first component (Figure 9(a)) reflect an evolution mode identical to the one described by the PCA component without rotation, with some differences like excesses, less accentuated from 1918 to 1953 in contrast with the other three PCs.

C. Spectral Analysis

It should be noted that the semi-arid character of northern Algeria, particularly the western zone, is partly defined by the changes in the general atmospheric circulation. Several studies connect precipitation compression to the North Atlantic Oscillation (NAO), which impacts the Mediterranean climate [31-36]. The phenomenon is studied quantitatively by the NAO index, which describes a normalized pressure difference between the measurements made in the Azores and Iceland. The index differs from year to year, but also shows a tendency to stagnate in one phase during long intervals [37]. Recently, its sign changed, mainly because of two concurrent trends observed during winter over the last three decades, leading towards a positive phase. These winters are related to higher than usual pressure in the subtropics and lower pressure in the Arctic. Thus, winters are dry and warm in Southern Europe, wet and warm in Northern Europe, and dry and cold in Greenland. On the other hand, during the negative periods of the NAO, winters are usually cold in Northern Europe, wet and humid in Southern Europe, and milder in Greenland. Climate anomalies combined with the NAO have effects on rainfall in North Africa, as demonstrated in [38-42]. The periodicity demonstrated for this part of the study area can also be tuned to the 25 years of the positive observed phase of the NAO (as it was a depiction of the correlation analysis).

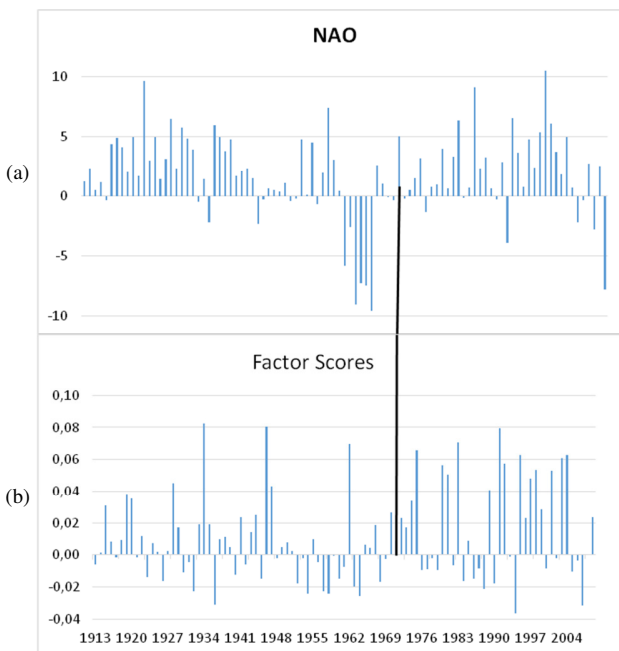


Fig. 9. Temporal evolution of the annual NAO index and the factorial scores PC1.

Thus, a study taking into account the observation period of 2005–2011 could reveal that the negative phase of NAO led to increased precipitation. From the middle of 1970's to 2000, the NAO annual index enters a positive phase, and the regional precipitation regime, represented by the first component, presents a decreasing trend. Furthermore, a negative association (Pearson's $r = 0$, Pearson's $r = 0.209$) was found

between the first component and NAO during 1975–2000. The association will be clear on a seasonal scale, as the NAO phenomenon affects winter precipitation.

X. CONCLUSION

The use of Principal Component Analysis (PCA) allowed us to identify 4 significant geographical regions with coherent precipitation variability showing the influence of two regimes in the investigated area: a central zone from the north toward the south of Algeria that is affected by the rainfall deficit and two lateral zones registering no deficits. The reliefs of the analyzed area are essential to the high mountain plateau type, and the noticed phenomena are less dependent on the intrinsic characteristics of the domain. However, this would require a considerable change of the meteorological variations over a wider area, determining the transit corridors of the rainy currents. It precedes the unique effect of the approach of Moroccan Atlas mountain range. The central region of the domain becomes the most targeted for climate change. Nonparametric statistical tests of the annual precipitation series show a weak trend at most of the studied stations in Algeria. The result is in line with the results received in several trend analysis studies. One of the suggested recommendations to describe wet and dry sequences precisely is the analysis of precipitation time scales over the years, which enable the study of possible changes in rainy and dry times.

REFERENCES

- [1] A. A. Mahessar *et al.*, "Rainfall Analysis for Hyderabad and Nawabshah, Sindh, Pakistan," *Engineering, Technology & Applied Science Research*, vol. 10, no. 6, pp. 6597–6602, Dec. 2020, <https://doi.org/10.48084/etasr.3923>.
- [2] M. Iturbide *et al.*, "An update of IPCC climate reference regions for subcontinental analysis of climate model data: definition and aggregated datasets," *Earth System Science Data*, vol. 12, no. 4, pp. 2959–2970, Nov. 2020, <https://doi.org/10.5194/essd-12-2959-2020>.
- [3] R. Mahmood, S. Jia, and W. Zhu, "Analysis of climate variability, trends, and prediction in the most active parts of the Lake Chad basin, Africa," *Scientific Reports*, vol. 9, no. 1, Apr. 2019, Art. no. 6317, <https://doi.org/10.1038/s41598-019-42811-9>.
- [4] S. Taibi, M. Meddi, D. Souag, and G. Mahe, "Evolution et regionalisation des precipitations au nord de l'Algerie (1936–2009)," in *Climate and land surface changes in hydrology*, Gothenburg, Sweden, Jul. 2013, vol. 359, pp. 191–197.
- [5] P. Hubert and J.-P. Carboneil, "Approche statistique de l'aridification de l'Afrique de l'Ouest," *Journal of Hydrology*, vol. 95, no. 1, pp. 165–183, Nov. 1987, [https://doi.org/10.1016/0022-1694\(87\)90123-5](https://doi.org/10.1016/0022-1694(87)90123-5).
- [6] P. Hubert, J. P. Carboneil, and A. Chaouche, "Segmentation des series hydrometeorologiques — application a des series de precipitations et de debits de l'afrique de l'ouest," *Journal of Hydrology*, vol. 110, no. 3, pp. 349–367, Oct. 1989, [https://doi.org/10.1016/0022-1694\(89\)90197-2](https://doi.org/10.1016/0022-1694(89)90197-2).
- [7] A. Gustard, "Variations spatio-temporelles des regimes pluviometriques et hydrologiques en Afrique centrale du debut du sie`cle a` nos jours," in *FRIEND'97: Regional Hydrology: Concepts and Models for Sustainable Water Resource Management*, Wallingford, OXF, UK: International Association of Hydrological Sciences, 1997, pp. 257–263.
- [8] S. R. Samo, N. Bhatti, A. Saand, M. A. Keerio, and D. K. Bangwar, "Temporal Analysis of Temperature and Precipitation Trends in Shaheed Benazir Abad Sindh, Pakistan," *Engineering, Technology & Applied Science Research*, vol. 7, no. 6, pp. 2171–2176, Dec. 2017, <https://doi.org/10.48084/etasr.1388>.
- [9] B. Alves, D. B. Angnuureng, P. Morand, and R. Almar, "A review on coastal erosion and flooding risks and best management practices in West Africa: what has been done and should be done," *Journal of*

- Coastal Conservation*, vol. 24, no. 3, Jun. 2020, Art. no. 38, <https://doi.org/10.1007/s11852-020-00755-7>.
- [10] Z. Nouaceur, "La reprise des pluies et la recrudescence des inondations en Afrique de l'Ouest sahelienne," *Physio-Geo. Geographie physique et environnement*, vol. 15, pp. 89–109, Mar. 2020, <https://doi.org/10.4000/physio-geo.10966>.
- [11] M. Sidibe, "Past and future hydroclimatic variability over West and Central Africa and their teleconnections," Ph.D. dissertation, Coventry University, Coventry, England, 2019.
- [12] P. Coratza and C. Parenti, "Controlling Factors of Badland Morphological Changes in the Emilia Apennines (Northern Italy)," *Water*, vol. 13, no. 4, Jan. 2021, Art. no. 539, <https://doi.org/10.3390/w13040539>.
- [13] A. Greco, D. L. De Luca, and E. Avolio, "Heavy Precipitation Systems in Calabria Region (Southern Italy): High-Resolution Observed Rainfall and Large-Scale Atmospheric Pattern Analysis," *Water*, vol. 12, no. 5, May 2020, Art. no. 1468, <https://doi.org/10.3390/w12051468>.
- [14] H. B. Abubakar, S. W. Newete, and M. C. Scholes, "Drought Characterization and Trend Detection Using the Reconnaissance Drought Index for Setsoto Municipality of the Free State Province of South Africa and the Impact on Maize Yield," *Water*, vol. 12, no. 11, Nov. 2020, Art. no. 2993, <https://doi.org/10.3390/w12112993>.
- [15] Y. Ban, P. Zhang, A. Nascetti, A. R. Bevington, and M. A. Wulder, "Near Real-Time Wildfire Progression Monitoring with Sentinel-1 SAR Time Series and Deep Learning," *Scientific Reports*, vol. 10, no. 1, Jan. 2020, Art. no. 1322, <https://doi.org/10.1038/s41598-019-56967-x>.
- [16] A. Douguedroit and C. Norrant, "Annual and Seasonal Century Scale Trends of the Precipitation in the Mediterranean Area During the Twentieth Century," in *Mediterranean Climate: Variability and Trends*, H.-J. Bolle, Ed. Berlin, Heidelberg: Springer, 2003, pp. 159–163.
- [17] A. J. O'Donnell, M. Renton, K. J. Allen, and P. F. Grierson, "Tree growth responses to temporal variation in rainfall differ across a continental-scale climatic gradient," *PLOS ONE*, vol. 16, no. 5, 2021, Art. no. e0249959, <https://doi.org/10.1371/journal.pone.0249959>.
- [18] V. Homar, C. Ramis, R. Romero, and S. Alonso, "Recent trends in temperature and precipitation over the Balearic Islands (Spain)," *Climatic Change*, vol. 98, no. 1, Sep. 2009, Art. no. 199, <https://doi.org/10.1007/s10584-009-9664-5>.
- [19] H. B. Mann, "Nonparametric Tests Against Trend," *Econometrica*, vol. 13, no. 3, pp. 245–259, 1945, <https://doi.org/10.2307/1907187>.
- [20] M. G. Kendall, *Rank correlation methods*. London, UK: Griffin, 1948.
- [21] V. Totaro, A. Gioia, and V. Iacobellis, "Numerical investigation on the power of parametric and nonparametric tests for trend detection in annual maximum series," *Hydrology and Earth System Sciences*, vol. 24, no. 1, pp. 473–488, Jan. 2020, <https://doi.org/10.5194/hess-24-473-2020>.
- [22] P. Pathak, A. Kalra, S. Ahmad, and M. Bernardez, "Wavelet-Aided Analysis to Estimate Seasonal Variability and Dominant Periodicities in Temperature, Precipitation, and Streamflow in the Midwestern United States," *Water Resources Management*, vol. 30, no. 13, pp. 4649–4665, Oct. 2016, <https://doi.org/10.1007/s11269-016-1445-0>.
- [23] E. L. Lehmann and H. J. D'Abrera, *Nonparametrics: Statistical methods based on ranks*. Oxford, England: Holden-Day, 1975.
- [24] P. Sneyers, *Sur l'analyse statistique des séries d'observations*. Geneva, Switzerland: OMM, 1990.
- [25] P. J. Pilon, R. Condie, and K. D. Harvey, "Consolidated Frequency Analysis Package, 1985," in *Cfa User Manual for Version 1: Dec Pro Series*, Ottawa, Canada: Environment Canada, Water Resources Branch, 1985.
- [26] A. I. McLeod, K. W. Hipel, and F. Comancho, "Trend Assessment of Water Quality Time Series," *Journal of the American Water Resources Association*, vol. 19, pp. 537–547, Aug. 1983, <https://doi.org/10.1111/j.1752-1688.1983.tb02768.x>.
- [27] K. W. Hipel and A. I. McLeod, *Time Series Modelling of Water Resources and Environmental Systems*. Amsterdam, Netherlands: Elsevier, 1994.
- [28] A. N. Pettitt, "A Non-Parametric Approach to the Change-Point Problem," *Journal of the Royal Statistical Society: Series C (Applied Statistics)*, vol. 28, no. 2, pp. 126–135, 1979, <https://doi.org/10.2307/2346729>.
- [29] M. B. Richman, "Rotation of principal components," *Journal of Climatology*, vol. 6, no. 3, pp. 293–335, 1986, <https://doi.org/10.1002/joc.3370060305>.
- [30] P. Camberlin, "Les précipitations dans la corne orientale de l'Afrique : climatologie, variabilité et connexions avec quelques indicateurs océano-atmosphériques," Ph.D. dissertation, University of Burgundy, Dijon, France, 1994.
- [31] M. Beniston, M. Rebetez, F. Giorgi, and M. R. Marinucci, "An analysis of regional climate change in Switzerland," *Theoretical and Applied Climatology*, vol. 49, no. 3, pp. 135–159, Sep. 1994, <https://doi.org/10.1007/BF00865530>.
- [32] I. F. Trigo, T. D. Davies, and G. R. Bigg, "Decline in Mediterranean rainfall caused by weakening of Mediterranean cyclones," *Geophysical Research Letters*, vol. 27, no. 18, pp. 2913–2916, 2000, <https://doi.org/10.1029/2000GL011526>.
- [33] R. M. Trigo *et al.*, "The Impact of North Atlantic Wind and Cyclone Trends on European Precipitation and Significant Wave Height in the Atlantic," *Annals of the New York Academy of Sciences*, vol. 1146, no. 1, pp. 212–234, 2008, <https://doi.org/10.1196/annals.1446.014>.
- [34] N. C. Nebout, V. Bout-Roumzeilles, I. Dormoy, and O. Peyron, "Secheresses recurrentes en Mediterranee au cours des derniers 50 000 ans," *Science et changements planétaires / Secheresse*, vol. 20, no. 2, pp. 210–216, Apr. 2009, <https://doi.org/10.1684/sec.2009.0181>.
- [35] A.-E. Briciu and D. Mihaila, "Wavelet analysis of some rivers in SE Europe and selected climate indices," *Environmental Monitoring and Assessment*, vol. 186, no. 10, pp. 6263–6286, Oct. 2014, <https://doi.org/10.1007/s10661-014-3853-z>.
- [36] C. Sun, J. Li, R. Ding, and Z. Jin, "Cold season Africa–Asia multidecadal teleconnection pattern and its relation to the Atlantic multidecadal variability," *Climate Dynamics*, vol. 48, no. 11, pp. 3903–3918, Jun. 2017, <https://doi.org/10.1007/s00382-016-3309-y>.
- [37] J. W. Hurrell, "Decadal Trends in the North Atlantic Oscillation: Regional Temperatures and Precipitation," *Science*, vol. 269, no. 5224, pp. 676–679, Aug. 1995, <https://doi.org/10.1126/science.269.5224.676>.
- [38] P. J. Lamb, "Chapter 5: West Africa," in *Teleconnections Linking Worldwide Climate Anomalies. Scientific Basis and Societal Impact*, M. H. Glantz, R. W. Katz, and M. Nicholls, Eds. New York, NY, USA: Cambridge University Press, 1991.
- [39] A. Khaldi, "Impacts de la secheresse sur le regime des ecoulements souterrains dans les massifs calcaires de l'Ouest Algerien Monts de Tlemcen - Saïda," Ph.D. dissertation, University of Oran, Oran, Algeria, 2005.
- [40] M. M. Meddi, A. A. Assani, and H. Meddi, "Temporal Variability of Annual Rainfall in the Macta and Tafna Catchments, Northwestern Algeria," *Water Resources Management*, vol. 24, no. 14, pp. 3817–3833, Nov. 2010, <https://doi.org/10.1007/s11269-010-9635-7>.
- [41] L. Brandimarte, G. Di Baldassarre, G. Bruni, P. D'Odorico, and A. Montanari, "Relation Between the North-Atlantic Oscillation and Hydroclimatic Conditions in Mediterranean Areas," *Water Resources Management*, vol. 25, no. 5, pp. 1269–1279, Mar. 2011, <https://doi.org/10.1007/s11269-010-9742-5>.
- [42] A. N. Laghari, W. Rauch, and M. A. Soomro, "A Hydrological Response Analysis Considering Climatic Variability: Case Study of Hunza Catchment," *Engineering, Technology & Applied Science Research*, vol. 8, no. 3, pp. 2981–2984, Jun. 2018, <https://doi.org/10.48084/etasr.2056>.